

# DISCHARGE GEOMETRY BEHAVIOR IN A POSITIVE CORONA SIMULATION IN A NON – UNIFORM COAXIAL ARRANGEMENT

LILIANA ARÉVALO<sup>1\*</sup>, MARLEY BECERRA<sup>2</sup> FRANCISCO ROMÁN<sup>1</sup>

Electromagnetic Compatibility Research Group EMC – UN

<sup>1</sup>National University of Colombia, Bogotá, Colombia;

<sup>2</sup>Uppsala University, Uppsala, Sweden.

Ciudad Universitaria Unidad Camilo Torres Bloque 4 Of. 702 Bogotá – Colombia  
COLOMBIA - SWEDEN

<http://www.emc-un.unal.edu.co>

## Abstract:

The results of numerical simulation of the positive corona development in atmospheric air in a needle placed in the inner cylinder of a cylindrical coaxial arrangement are presented. The Poisson's equation was simultaneously solved with the continuity equations for electrons, positive ions and negative ions, including the effects of ionization, attachment, recombination and photo ionization. The values of electric field and corona current are shown and compared with the experimental ones. Comparisons of two different discharge channels are shown. A truncated cones and a cylindrical discharge channel were investigated.

## Key-Words:

Positive corona, streamer, continuity equations, Poisson equation, particles density, numerical techniques, photoionization, attachment, recombination

## 1. The theoretical “equations and parameters”

The discharge geometry is an assumption in the corona effect calculation. Its geometric form has been obtained of experimental observations. Many experimental results have shown that the discharge presents a filamentary geometry [5]. Nevertheless, some authors have shown that the geometry discharge in low pressures is not quite filamentary, in some cases, it has been seen that the discharge channel on the cathode is twice the radius of the anode side. In order to determine and compare which one is the discharge geometry, in this arrangement truncated cone geometry has been chosen. Electron, positive and negative – ion continuity equations including ionization, attachment recombination and photoionization were simultaneously solved with Poisson's equation. The solutions of the convective flow of particles were obtained using a Flux – corrected – Transport algorithm [15, 16].

The coupled continuity equations for electrons, positive ions, and negative ions are:

$$\frac{\partial N_e}{\partial t} = S + N_e \alpha |W_e| - N_e \eta |W_e| - N_e N_p \beta - \frac{\partial(N_e W_e)}{\partial x} + \frac{\partial}{\partial x} \left( D \frac{\partial N_e}{\partial x} \right) \quad (1)$$

$$\frac{\partial N_p}{\partial t} = S + N_e \alpha |W_e| - N_e N_p \beta - N_n N_p \beta - \frac{\partial(N_p W_p)}{\partial x} \quad (2)$$

$$\frac{\partial N_n}{\partial t} = N_e \eta |W_e| - N_n N_p \beta - \frac{\partial(N_n W_n)}{\partial x} \quad (3)$$

$$\frac{\partial N_m^i}{\partial t} = \delta^i W_e N_e - \frac{N_m^i}{\tau_m^i} \quad (4)$$

$$\frac{\partial N_{ph}^i(r, \theta, \phi, t)}{\partial t} = \frac{N_m^i(r, t)}{4\pi\tau_m^i} - \mu^i c N_{ph}^i(r, \theta, \phi, t) - \zeta \frac{\partial N_{ph}^i(r, \theta, \phi, t)}{\partial r} \quad (5)$$

Where  $t$  is time,  $x$  the distance from the anode;  $N_e$ ,  $N_p$ ,  $N_n$  and  $N_m$ , are the respective electron, positive ion, negative ion and molecule densities; and  $W_e$ ,  $W_p$  and  $W_n$  the respective electron, positive ion and negative ion drift velocities. The superscript  $i$  denotes the  $i$ th excitation coefficient of a molecule level and also photons emitted from that level.  $\delta^i$  is the excitation coefficient level,  $\mu^i$  and  $\tau_m^i$  are the respective photons absorption coefficient and the excited molecule lifetime from that level.  $N_{ph}(r, \theta, \phi, t)$  is the photon density at  $\mathbf{r}$  in real space per steradian in the direction of velocity in polar coordinates  $(\theta, \phi)$ . The symbols  $\alpha$ ,  $\eta$ ,  $\beta$ , and  $D$

denote the ionization, attachment, recombination and electron diffusion coefficients respectively,  $c$  is the speed of light,  $\zeta$  the photon velocity and  $S$  is the source term due to photoionization.

Poisson's equation is:

$$\nabla^2 \phi = -\frac{e}{\epsilon} (N_p - N_e - N_n) \quad (6)$$

where:  $\epsilon$  is the dielectric constant,  $e$  the electron charge and  $\phi$  the electric potential. The electric field,  $E$ , is computed as:  $E = -\nabla \phi$ . (7)

The current  $I$ , in the external circuit, due to the motion of electrons and ions between the electrodes, was calculated using Sato's equation [14]:

$$I = \frac{Ae}{V_a} \int_0^d \left( N_p W_p - N_n W_n - N_e W_e + D \frac{\partial N_e}{\partial x} \right) E_L \cdot dx \quad (8)$$

where:  $V_a$  is the applied voltage,  $A$  is the cross sectional area of the discharge channel and  $E_L$  is the LaPlacian electric field.

The background electric field  $E_{back}$  was calculated with the values obtained using the program Ansys®, in a free space charge condition. The electric field due to the spatial charge  $E_c$  was calculated using "the disc method" or better known as "one and one – half method" [11]. Thus, the axial total electric field  $E(x)$  at the point  $x$  was calculated as:

$$E(x) = E_{back}(x) + E_c(x) \quad (9)$$

To start the computation at  $t_0$ , an electron density was considered ( $10^3 \text{ cm}^{-3}$ ) in a Gaussian distribution. To keep the calculation time between reasonable limits, a uniform  $20\mu\text{m}$  mesh with a total number of axial 1500 elements was used to represent the 4 cm interelectrode gap distance. For the electric field calculation, in the cylindrical channel discharge simulation a  $4\mu\text{m}$  radius was considered, and for the 2D simulation a truncated cone with  $0.4\mu\text{m}$  radius on the anode side and a  $0.15\text{mm}$  on the cathode side.

## 2. Experimental Set-Up and Results [17, 18]

The air streamer development calculations were performed at the atmospheric conditions of Bogotá, Colombia (2600m o.s.l.). The experimental setup was a coaxial cylindrical arrangement with a corona-electrode

radially placed on the inner electrode surface. The corona-electrode was a brass rod terminated on a  $0.15\text{mm}$  radius of curvature hyperbolical tip. A  $5.9 \text{ kV}$  voltage was applied to the external cylindrical electrode, while the internal cylinder was earthed across a measuring resistor. Current was measured with a LeCroy oscilloscope LC574AM. The measured current is shown in Fig. 1.

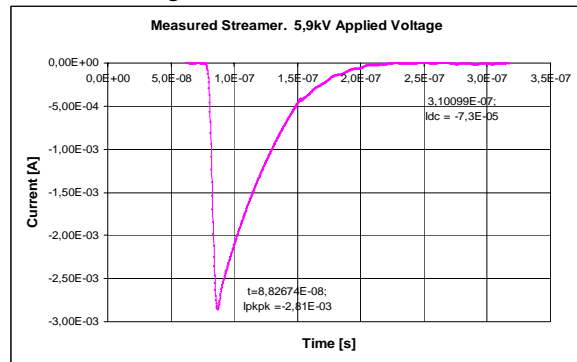


Fig. 1. Measured streamer current when a DC voltage amplitude of  $5.9\text{kV}$  was applied to the external cylindrical electrode.

### 2.1. Simulation Results

Fig. 2 shows that the waveforms obtained for both geometries are the same but the current magnitudes are different. For the conical simulation the current peak is  $596\mu\text{A}$ , meanwhile in the cylindrical simulation is  $2.81\text{mA}$ . The direct current component has the same behavior, for the conical discharge geometry is  $68\mu\text{A}$  and in the cylindrical geometry is  $110\mu\text{A}$ . It can be concluded that the best-fit discharge geometry is the cylindrical, and then the discharge has a filamentary geometry.

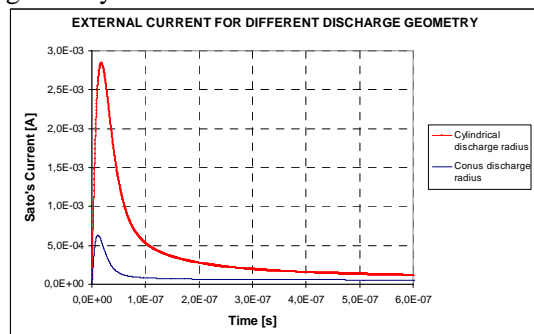


Fig. 2. Current behavior for different discharge geometry. Notice that peak and direct current values are different for each case.

Different time stages were compared, the initial streamer formation (13ns), the slow streamer propagation (45ns), the streamer decay (150ns) and the streamer termination (645ns). As all figures show the particles density distributions are similar, but they differ in magnitudes. Additionally, the particles move along the interelectrode gap space at almost the same velocity.

In the first stage, Fig.3, electrons and ionic particles are located in the same interelectrode gap space for both geometries. In the cylindrical discharge channel the particles densities are ~4 times higher than the particles behavior for the conical geometry. In both geometries, the most important charge is the positive ion density. Comparisons of the maximum and minimum magnitudes of the different particles show that in the conical geometry the reasons between positive and negative ion densities and positive ion and electron densities are higher than in the cylindrical geometry. The electron density in the conical geometry is 0.51 times the positive ion density; meanwhile in the cylindrical geometry electron density is 0.35 times the positive ion density.

The negative ion density presents the same behavior, negative ion density in the conical geometry is 0.6 times the positive ion density, while in the cylindrical geometry negative ion density is 0.4 times positive ion density. The positive ion density is located in the tip of the point for both geometries. The conical discharge radius is smaller in this region than in the cylindrical channel, and then the positive ion density is smaller in the conical geometry than in the cylindrical one.

In the slow streamer propagation stage 45ns (Fig. 4), the particles densities differ 4 times between the cylindrical and the conical discharge channel. Ionic density differences maintain: negative ion density in the conical geometry is 0.5 times the positive ion density, meanwhile in the cylindrical geometry negative ion density is 0.4 times the positive ion density. Electron density difference has reduced and electrons are 0.2 times positive ion density in both geometries. This means that electron recombination and attachment takes place faster in the conical geometry than in the cylindrical geometry. Furthermore, Fig. 4 shows that electrons in the conical geometry move faster than in the cylindrical geometry.

In latter times 150ns (Fig. 5.), streamer decay stage, particles densities are located in the same interelectrode gap space, positive ion density is still the most important charge density and three different regions are visible: positive ion density location, negative ion density region and electron density which is moving through the interelectrode gap space. Electron densities maximum between both geometries are located in different interelectrode regions as in the past stage; this is probably due to the larger radius in the conical discharge channel than in the cylindrical.

In the streamer termination 645ns (Fig. 6), ionic charge density is the most important particle density in the interelectrode gap space, electron density is only the 1% of the total charge along the gap. Cylindrical geometry particles density is 4 times conical geometry particles density. In the past stage, in the conical geometry electrons were faster than electrons in the cylindrical geometry; in this stage electrons slow down and are located almost in the same interelectrode gap space

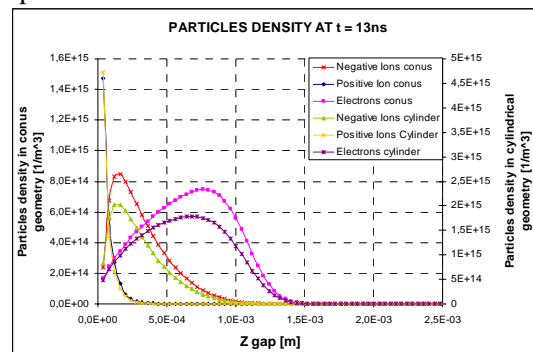


Fig. 3. Particles density at 13ns. Notice that particle distributions are equal in both cases but their magnitudes are different.

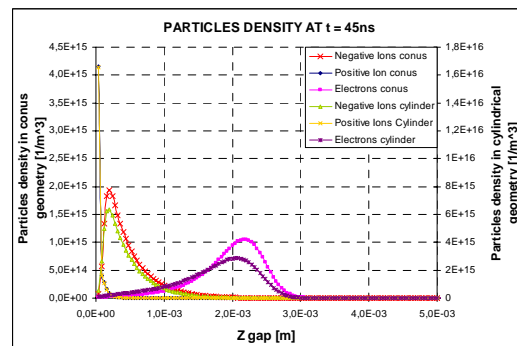


Fig. 4. Particles density at 45ns. Notice that cylindrical discharge channel has a higher particles density than the conical discharge channel.

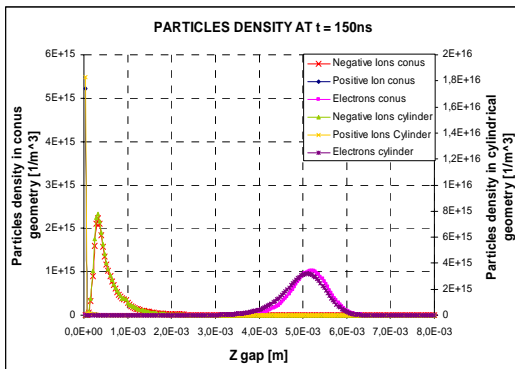


Fig. 5. Particles density at 150ns. Notice that there are three different defined regions: the positive discharge region, negative discharge region and the electrons moving through the cathode.

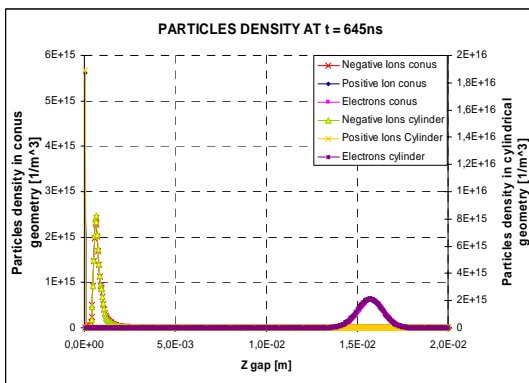


Fig. 6. Particles density at 650ns. Notice that ionic charge is the most important charge particle in the interelectrode gap space, electrons move slowly along the interelectrode gap space.

### 3. Discussion

When a conical discharge channel is used, the positive ion density became smaller than in the cylindrical discharge geometry, due to the smaller discharge radius of the conical geometry a fewer ionization and recombination region for process positive ion generation will exist. In a truncated cone the radius is increasing the region where attachment process will take place and the negative ions density is higher than in the cylindrical geometry. Additionally that is why negative ion density at initial time is comparable with positive ion density in the conical geometry.

The peak current in the conical discharge geometry is

not high as the peak current of a cylindrical discharge channel. Electrons are responsible of the current grown and its density depends of the discharge channel, at the initial stage in conical discharge geometry the small discharge radius does not permit that electron density grows high enough to produce a higher external current.

The initial current pulse could be explained as the electron density growth during the first time stage ( $0 < t < 19\text{ns}$ ). This fast electronic growth is due to the initial avalanches in the high electric field region.

After 19ns positive and negative ion densities became the most significant part of the current. As positive ions are the heaviest, they can be considered almost static along the streamer development process. Negative ion charge density increases with time but its velocity along the interelectrode gap space is very slow. Therefore, the ionic charge is the most important charge to be considered when the current is decreasing. Therefore, it can be concluded that during the streamer-decay and -termination stages an ionic current will develop.

As the calculations have shown, the most important input variables are the gas parameters and discharge channel geometry.

### 4. Conclusions

- (1) The calculations gave detailed predictions of particles behavior as function of time and interelectrode gap space. Spatial resolution over the electrode separation of 40mm is one of the most important parameters to obtain an accurate particle behavior.
- (2) In the coaxial arrangement, the geometrical discharge form is cylindrical; this means that the discharge is filamentary. The discharge geometry determines the particles density and then the external circuit magnitude. However, it does not change the particles behavior or waveform in the interelectrode gap space.
- (3) The performed calculations were essential to understand the following aspects of the positive corona discharge:
  - The fast current impulse rise time and amplitude were mainly explained by the electron density

performance, while the essential secondary process for the streamer development and propagation was the photoionization process.

- The main cause for the DC current component was the ionic current due to the negative and positive ion densities.

(4) Comparing the measured current with the simulated with the cylindrical channel it can be concluded, that the high electric field left along the gap space makes possible that another streamer will develop before the positive ion density is absorbed by the anode. Due to the fact that another streamer was measured after 700ns, the positive ion density it is not able to reach the anode.

## Acknowledgments

The authors would like to thank Universidad Nacional de Colombia and Colciencias for supporting the present research work (RC number 470 – 2003).

### References:

- [1] Essam Nasser. Fundamentals of Plasma Gaseous. Wiley – Interscience 1971
- [2] J. Meek and J. Craggs. Electrical Breakdown of Gases. Wiley – Interscience 1988
- [3] Lan Gao. Characteristics of Streamer Discharges in Air and Along Insulating Surfaces. Uppsala University 2000
- [4] S. Badaloni and I. Gallimberti. Basic Data of Air Discharges. Universita' di Padova 1972
- [5] Morrow, Lowke. . Streamer Propagation in Air. *J. Phys. D* 30 614 – 627. 1997
- [6] Allen, Ghaffar *J. Phys. C. Appl.* 28 338-343. 1995
- [7] Yoshida K. H. Tagashira. Computer Simulation of a Nitrogen Discharge at High Overvoltages. *J Phys. D.* Vol 9, 1976
- [8] I. Odrobina and M. Cernak. Numerical simulation of streamer – cathode interaction. *J. Appl. Phys.* 78. 1995
- [9] J. Kennedy, Megens and M. Wetzler. Cathode Photoelectron Emission During A Gas Discharge In N<sub>2</sub> And Dry Air. *IEEE ISEI* 1994
- [10] S. Okabe, T. Hara and F. Takaaki. Simulation Of Positive Corona Discharge In Sf<sub>6</sub> Gas By Multichannel Model. *IEEE ISEI* 1996
- [11] A. Davies, C. Evans. Field distortion in gaseous discharges between parallel – plate electrodes. *Proc. IEE*, Vol 124, N° 2, 1977
- [12] Legler W. *Z Phys.* 173, 169 - 183. 1963
- [13] Penney G. W. and Hummert G. Photoionization measurements in air, oxygen and nitrogen. *J Appl. Phys.* 41 572 – 577. 1970
- [14] N. Sato. Discharge Current Induced By The Motion Of Charged Particles. *J Phys. D: Appl. Phys.* 13, L3. 1980
- [15] Boris, Book. Flux corrected transport. I. Shasta, a fluid transport algorithm that works. *J. Comp Phys.* 11, 38 – 69. 1973
- [16] Zalesak. Fully Multidimensional Flux – Corrected Transport Algorithms For Fluids. *J of Comp Phys* 31, 363 – 378. 1979
- [17] Arévalo, Díaz, López, Gómez, and Román. Corona Current Impedance...., *27th ICLP 2004*.
- [18] L. Arévalo, O. Díaz and F. Román Adding negative corona currents produced by independent electrodes. *XIIIth International Symposium on High Voltage Engineering.* 2003.